contributions; the latter type can be mixed with Mo d out-of-plane orbitals to give Mo–S π character as has been described for other $M_2(\mu\text{-}S)_2$ systems.[2,46–50] Two such Mo–S π interactions are allowed for radical $Mo_2S^{\bullet}$ and anion Mo_2S^-, which would allow an average π bond order of 0.5. That the chemistry is primarily sulfur-based in $Mo_2S^{\bullet}$ and in Mo_2S^- suggests that one of the S p (Mo–S π) orbitals may be the SOMO or HOMO therein; for $Mo_2S^{\bullet}$ this results in a diminished π interaction. A π-type radical has been described for the sulfur bridge of $[M_2(CO)_{10}S]^-$ (M = Cr, W).[51] When one bridge sulfur is bonded to a third atom in the Mo_2SZ compounds, the energy of its S p orbital is altered due to involvement in σ bond formation and the π participation is lost; the Mo–S π interaction at the second sulfur is concomitantly strengthened. This is supported by crystal structure results for several derivatives: Mo–S(dicoordinate) and Mo–S(tricoordinate) bridge bond distances differ by 0.09–0.11 Å.[12,52–54] The strengthening of the Mo–S(dicoordinate) π interaction accounts for the effective passivation of the second sulfur site. Similar descriptions have been expressed for other metallosulfur dimers.[2,48] For current derivatives with a tricoordinate bridge, the Mo–Mo σ orbital may then be the HOMO.

The high-wavelength S–S photohomolysis of Mo_2SSMo_2 and Mo_2SSR (R = aryl) suggests that the S–S σ^* may be the LUMO in these specific compounds, closely followed then by the aforementioned Mo–L π^* and Mo–Mo σ^* orbitals. The transition involved in the photohomolysis may then involve Mo–Mo $\sigma \rightarrow$ S–S σ^*. For Mo_2SSR (R = alkyl) derivatives, the stronger S–S bond leads to a substantially higher S–S σ^* orbital energy and a photolysis transition in the ultraviolet. The overall picture suggests that the Mo_2S–S bond is lower in energy than organic RS–S bonds for R = alkyl; for R = aryl, the comparison is ambiguous. The corollary is that $Mo_2S^{\bullet}$ is a more stabilized radical than $RS^{\bullet}$, R = alkyl.

These considerations are of interesting consequence to the tetrasulfide $Mo_2SSSSMo_2$. Alkyl tetrasulfides are more homolytically sensitive at internal RSS–SSR bonds than at RS–SSSR bonds, due again to differences in bond energies.[13,33,34,55] Presently, however, the decreased energy of Mo_2S–S bonds is proposed to reverse that behavior, such that Mo_2S–$SSSMo_2$ bonds are a weaker link than the Mo_2SS–$SSMo_2$ bonds. Preferential photohomolysis of Mo_2S–$SSSMo_2$ over Mo_2SS–$SSMo_2$ bonds would indeed account for the observed production of Mo_2SSMo_2 and the absence of trisulfide Mo_2SSSMo_2. This would also suggest that the observed polysulfides $Mo_2SSS_xSSMo_2$, at least initially, are of even-numbered sulfur chains, since these result from combination of two odd-numbered sulfur chain radicals.

Acknowledgment. This work was supported by research awards from the National Science Foundation and the Kentucky EPSCoR Program.

---

(46) Szterenberg, L.; Jezowska-Trzebiatowska, B. *Inorg. Chim. Acta* **1982**, *59*, 141.

(47) Müller, A.; Jostes, R.; Eltzner, W.; Nie, C.-S.; Diemann, E.; Bögge, H.; Zimmermann, M.; Dartmann, M.; Reinsch-Vogell, U.; Che, S.; Cyvin, S. J.; Cyvin, B. N. *Inorg. Chem.* **1985**, *24*, 2872.

(48) Hor, T. S. A.; Tan, A. L. C. *Inorg. Chim. Acta* **1988**, *142*, 173.

(49) Weberg, R. T.; Haltiwanger, R. C.; Rakowski DuBois, M. *New J. Chem.* **1988**, *12*, 361.

(50) Coucouvanis, D.; Hadjikyriacou, A.; Toupadakis, A.; Koo, S.-M.; Ileperuma, O.; Draganjac, M.; Salifoglou, A. *Inorg. Chem.* **1991**, *30*, 754.

(51) Hynes, R. C.; Preston, K. F.; Springs, J. J.; Williams, A. J. *Organometallics* **1991**, *10*, 180.

(52) Noble, M. E.; Folting, K.; Huffman, J. C.; Wentworth, R. A. D. *Inorg. Chem.* **1984**, *23*, 631.

(53) Noble, M. E.; Williams, D. E. *Inorg. Chem.* **1988**, *27*, 749.

(54) Pelati, J. E.; Huffman, J. C.; Wentworth, R. A. D. *Inorg. Chem.* **1988**, *27*, 2194.

(55) Burkey, T. J.; Hawari, J. A.; Lossing, F. P.; Lusztyk, J.; Sutcliffe, R.; Griller, D. *J. Org. Chem.* **1985**, *50*, 4966.

Rotational Isomerism and Fluxional Behavior of Bis(carbon dioxide) Adducts of Molybdenum

Ernesto Carmona,*,[1a] Andrew K. Hughes,[1b] Miguel A. Muñoz,[1a] Dermot M. O'Hare,[1b] Pedro J. Pérez,[1a] and Manuel L. Poveda[1a]

Contribution from the Departamento de Química Inorgánica-Instituto de Ciencia de Materiales, Facultad de Química, Universidad de Sevilla-CSIC, 41071 Sevilla, Spain, and Inorganic Chemistry Laboratory, South Parks Road, Oxford OX1 3QR, England. *Received May 28, 1991*

Abstract: The exchange reactions involving the bis(carbon dioxide) complex *trans*-$Mo(CO_2)_2(PMe_3)_4$ (**1**) and chelating phosphines P–P ($Me_2PCH_2PMe_2$, dmpm; $Me_2PCH_2CH_2PMe_2$, dmpe; $Et_2PCH_2CH_2PEt_2$, depe; and $Ph_2PCH_2CH_2PPh_2$, dppe) and isocyanides, CNR, provide efficient routes to the new $(CO_2)_2$ adducts *trans*-$Mo(CO_2)_2(P\text{–}P)(PMe_3)_2$ (P–P = dmpe (**3a**), depe (**3b**), dmpm (**3c**), dppe (**3d**)), *trans*-$Mo(CO_2)_2(P\text{–}P)_2$ (P–P = dmpe (**4a**), depe (**4b**)), and *trans*-$Mo(CO_2)_2(depe)(PMe_3)(CNR)$ (R = Bu^t (**5a**), Cy (**5b**)). Due to the asymmetric nature of the coordinated CO_2 groups and to the existence of different ligands (PMe_3, P–P, CNR) in the plane perpendicular to the $O_2C\text{–}Mo\text{–}CO_2$ bond axis, several isomers arising from the different conformations of the CO_2 ligands are possible for each of the above type of complex. Their existence has been demonstrated by variable-temperature NMR spectroscopy, and they have furthermore been shown to interconvert in solution. Four nondissociative mechanisms have been considered for this exchange process, of which one that involves exchange of the coordinated and free oxygen atoms of one of the CO_2 ligands has been shown to be inoperative. Two rotational mechanisms, namely an independent rotation and a disrotatory motion, have also been excluded. A concerted rotation of the CO_2 groups in which both molecules rotate in the same direction is in accord with all the experimental results.

Carbon dioxide activation by transition-metal compounds continues to attract considerable attention.[2] An important part of these studies is the synthesis and characterization of M–CO_2 complexes that can be used as models for relevant steps in the

0002-7863/91/1513-9210$02.50/0

catalytic cycles foreseen for CO_2-based chemical processes. Among the few mononuclear transition-metal–carbon dioxide compounds that have been structurally characterized,[3] an interesting and rather unusual system is that based on molybdenum complexes of type A (alternatively represented as in **B**, where the triangle symbolizes the non-coordinated, i.e. the exo, C=O bond)

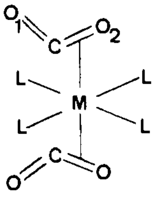

A

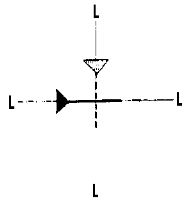

B

which contains two trans and mutually staggered molecules of CO_2 in an eclipsed conformation with respect to the *trans*-L–Mo–L vectors of the equatorial plane. Recent work from our laboratory[3d] has resulted in the synthesis and characterization of the complexes[4] *trans*-$Mo(CO_2)_2(PMe_3)_4$ (**1**) and *trans*-$Mo(CO_2)_2(PMe_3)_3(CNR)$ (**2**). These compounds exhibit fluxional NMR behavior that was not investigated at that time. Since the study of the fluxionality in these molecules could lead to a better understanding of the $M–CO_2$ interaction, an aspect of fundamental importance for the activation of CO_2 by transition-metal compounds, we have investigated the intimate nature of the mechanism responsible for the temperature dependence of the NMR spectra. A recent theoretical study, carried out by Sânchez-Marcos and co-workers with the model system *trans*-$Mo(CO_2)_2(PH_3)_4$, has shown that a low-energy process for the rotation of the coordinated CO_2 molecules is their concerted conrotatory motion around the $O_2C–Mo–CO_2$ axis. In order to experimentally check this claim and to unambiguously distinguish among the different mechanistic possibilities, we have carried out an investigation by dynamic NMR spectroscopy[6,7] of related complexes, less symmetric than **1**. With this aim in mind we have prepared the new $(CO_2)_2$ complexes[4] *trans*-$Mo(CO_2)_2(P–P)(PMe_3)_2$ (P–P = dmpe (**3a**), depe (**3b**), dmpm (**3c**), dppe (**3d**)), *trans*-$Mo(CO_2)_2(P–P)_2$ (P–P = dmpe (**4a**), depe (**4b**)), and *trans*-$Mo(CO_2)_2(depe)(PMe_3)(CNR)$ (R = Bu^t (**5a**), Cy (**5b**)). As described below, detailed, variable-temperature, multinuclear NMR studies carried out with complexes **2**–**5** show they exist in solution as mixtures of rotational isomers arising from the different conformations of the CO_2 ligands. These studies also show that the rotamers interconvert by means of a concerted mechanism in which the two molecules of CO_2 rotate synchronously in the same direction.[8]

Results

***trans*-$Mo(CO_2)_2(PMe_3)_4$ (1) and *trans*-$Mo(CO_2)_2(PMe_3)_3(CNR)$ (2) Complexes.** Although a detailed spectroscopic study of complex **1** that includes variable-temperature NMR measurements has already been reported,[3d] it is pertinent at this point to recall some relevant spectroscopic data. This is done here not only for the sake of completeness but also because it constitutes an excellent starting point for the discussion of the remaining $(CO_2)_2$ complexes to be presented in this and in the following sections. Complex **1** is a fluxional molecule for which spectroscopic data at low temperatures are consistent with a static structure of the type indicated in **B** above (or A, only one of the enantiomeric structures is shown), as evidenced by the observation of an AA′BB′ pattern in the $^{31}P\{^1H\}$ NMR spectrum (81 MHz, −60 °C, δ_A −3.2, δ_B 1.9; $^2J_{AB}$ = 144 Hz, $^2J_{AB'}$ = −18 Hz, $^2J_{AA'}$ = 14 Hz, $^2J_{BB'}$ = 23 Hz). Upon warming, a dynamic site-exchange of the ^{31}P nuclei takes place, and at temperatures around 50 °C (32.4 MHz), a singlet is observed which splits into a multiplet when **1** is enriched in $^{13}CO_2$ ($^2J_{CP}$ = 17 Hz).[3d]

For the *trans*-$Mo(CO_2)_2(PMe_3)_3(CNR)$ complexes (R = Bu^t (**2a**), Cy (**2b**)) only the fast exchange regime was originally studied.[3d] A dynamic NMR investigation has now demonstrated a rather complex behavior. For example, ^{31}P NMR studies reveal that complex **2a** exists in solution as a thermodynamic mixture of two isomers, **2a-I** and **2a-II**, in a 6:1 ratio (two AMX patterns at −90 °C in CD_3OD: major isomer δ_A −4.7, δ_M −2.6, δ_X 15.0; $^2J_{AM}$ = 23 Hz, $^2J_{AX}$ = 16 Hz, $^2J_{MX}$ = 148 Hz; minor isomer δ_A −4.8, δ_M 11.5, δ_X 16.5; $^2J_{AM}$ = 150, $^2J_{AX}$ = 20, $^2J_{MX}$ = 14 Hz). Since compounds **2** adopt structure **2-I** in the solid state,[3d] this structure can be reasonably proposed for the major isomer. In accord with this proposal, the $^{13}C\{^1H\}$ NMR spectrum of **2a**, ca. 30% enriched in $^{13}CO_2$, shows at −90 °C two doublets of triplets due to the non-equivalent CO_2 ligands in the major isomer **2a-I** with a uniquely large $^{13}C–^{31}P$ coupling constant (δ 210.7 (dt, $^2J_{CP}$ = 41, and 9 Hz), δ 213.5 (dt, $^2J_{CP}$ = 16, 10 Hz)).

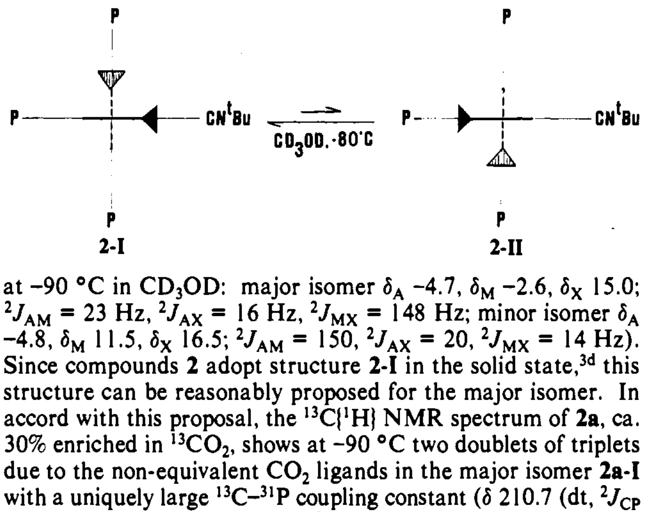

2-I **2-II**

At temperatures above −90 °C, the interconversion **2a-I** ⇌ **2a-II** becomes faster until at 45 °C a single $^{31}P\{^1H\}$ AX_2 pattern is observed (C_6D_6, δ_A −8.4, δ_X 0.4; $^2J_{AX}$ = 19 Hz). Due to the complexity of the system no attempt has been made to quantify the rate of exchange, but some qualitative information can be drawn from the analysis of the variable-temperature NMR spectra. Firstly, the trans phosphorus nuclei in rotamer **2a-I** exchange their environments faster than the corresponding pair in **2a-II**, which means that the site-exchange in rotamer **2a-I** is not necessarily correlated with the process responsible for the **2a-I** ⇌ **2a-II** interconversion. Secondly, a comparison of the chemical shifts of the ^{31}P nuclei in the fast-exchange limit with those corresponding to the low-temperature equilibrium mixture of **2a-I** and **2a-II** shows their ratio to be essentially temperature independent.

Compound **2b** (R = Cy) displays a similar behavior although in the slow-exchange limit two sets of closely spaced resonances, in a ca. 1:1 ratio, are observed for each of the rotamers **2b-I** and **2b-II** (whose ratio is again approximately 6:1). These are assigned to conformers derived from the equatorial–axial distribution of

---

(1) (a) Universidad de Sevilla-CSIC. (b) University of Oxford.

(2) For recent review on CO_2 chemistry see: (a) Walter, D. *Coord. Chem. Rev.* **1987**, *79*, 135. (b) Braunstein, P.; Matt, D.; Nobel, D. *Chem. Rev.* **1988**, *88*, 747. (c) Behr, A. *Carbon Dioxide Activation* by *Metal Complexes*; VCH Publishers: Weinheim, FRG, 1988. (d) Behr, A. *Angew. Chem., Int. Ed. Engl.* **1988**, *27*, 661.

(3) For mononuclear, structurally characterized $M–CO_2$ complexes see: (a) Gambarotta, S.; Arena, F.; Floriani, C.; Zanazzi, P. F. *J. Am. Chem. Soc.* **1982**, *104*, 5082. (b) Aresta, M.; Nobile, C. F.; Albano, V. G.; Forni, E.; Manassero, M. *J. Chem. Soc., Chem. Commun.* **1975**, 36. (c) Bristow, G. S.; Hitchcock, P. B.; Lappert, M. F. *J. Chem. Soc., Chem. Commun.* **1981**, 1145. (d) Alvarez, R.; Carmona, E.; Marín, J. M.; Poveda, M. L.; Gutiérrez-Puebla, E.; Monge, A. *J. Am. Chem. Soc.* **1986**, *108*, 2286. (e) Calabrese, J. C.; Herskovitz, T.; Kinney, J. B. *J. Am. Chem. Soc.* **1983**, *105*, 5914. (f) Gambarotta, S.; Floriani, C.; Chiesi-Villa, A.; Guastini, C. *J. Am. Chem. Soc.* **1985**, *107*, 2985.

(4) The prefix trans used in the formulation of these bis(carbon dioxide) complexes refers always to the geommetrical distribution of the CO_2 ligands.

(5) Sânchez-Marcos, E.; Caballol, R.; Trinquier, G.; Bartherlat, J. C. *J. Chem. Soc., Dalton Trans.* **1987**, 2373.

(6) (a) *Dynamic Nuclear Magnetic Resonance Spectroscopy*; Jackman, L. M., Cotton, F. A., Eds.; Academic Press: New York, 1975. (b) Sandström, J. *Dynamic NMR Spectroscopy*; Academic Press: New York, 1982. (c) Mann, B. E. In *Comprehensive Organometallic Chemistry*; Wilkinson, G., Stone, F. G. A., Abel, E. W., Eds.; Pergamon Press: Oxford, England, 1982; Vol. 3, Chapter 20.

(7) For recent related studies involving olefin ligands see: (a) Klein, H. F.; Helwig, M.; Koch, U.; Lull, G.; Tadic, M.; Krüger, C.; Hofmann, P. *Z. Naturforsh* **1988**, *43b*, 1427. (b) Albright, T. A. *Acc. Chem. Res.* **1982**, *15*, 149. (c) Wickenheiser, E. B.; Cullen, W. R. *Inorg. Chem.* **1990**, *29*, 4671. (d) Angermund, H.; Grevels, F.-W.; Moser, R.; Benn, R.; Krüger, C.; Romão, M. J. *Organometallics* **1988**, *7*, 1994.

(8) A preliminary account of part of this work has already appeared: Carmona, E.; Muñoz, M. A.; Pérez, P. J.; Poveda, M. L. *Organometallics* **1990**, *9*, 1337.

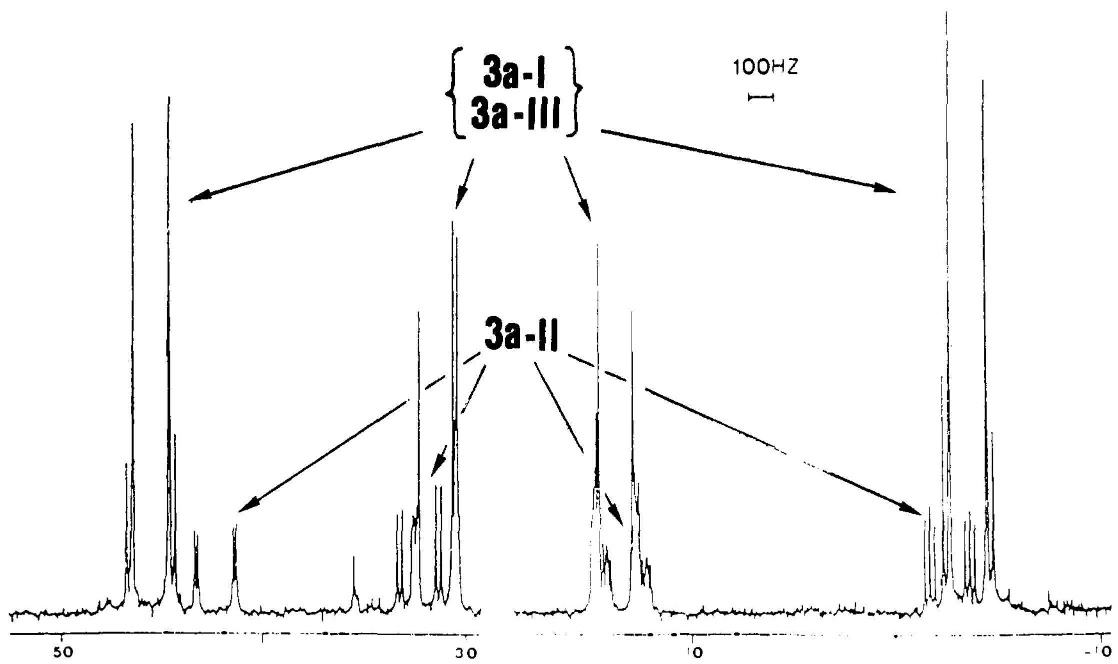

Figure 1. $^{31}P\{^1H\}$NMR spectrum (CD_3OD, −70 °C) of complex **3a**. Rotamers **3a-I** and **3a-III** cannot be unambiguously assigned (see text).

the cyclohexyl ring substituent.[9] Once again exchange of the trans ^{31}P nuclei is faster in **2b-I** than in **2b-II**.

***trans*-Mo(CO$_2$)$_2$(P–P)(PMe$_3$)$_2$ (3) Complexes.** The facility with which complex **1** undergoes PMe_3 exchange by other ligands[3d] can be used for the preparation of mixed-phosphine $(CO_2)_2$ adducts, as shown in eq 1. These phosphine-exchange reactions

$$\underset{\mathbf{1}}{trans\text{-}Mo(CO_2)_2(PMe_3)_4} \xrightarrow[\text{THF, 20 °C}]{\text{P–P}} trans\text{-}Mo(CO_2)_2(P\text{–}P)(PMe_3)_2 + 2PMe_3 \quad (1)$$

P–P = dmpe (**3a**), depe (**3b**),
dmpm (**3c**), dppe (**3d**)

are fast and require 30 min at room temperature for completion with the only exception being the dppe system for which stirring for 4 days at 20 °C is needed (at higher temperatures decomposition readily occurs). The new compounds have been characterized by microanalysis and IR and NMR spectroscopy. They are isolated as yellow crystalline solids, moderately stable to air in the solid state but much more sensitive in solution. Although almost insoluble in hexanes, they are fairly soluble in other common organic solvents. They display enhanced thermal stability as compared to **1** and, for example, complex **3a** can be heated in toluene at 90 °C without noticeable decomposition. Not unexpectedly, the CO_2 ligands give rise to IR absorptions at 1660, 1150, and 1100 cm^{-1} that compare well with those reported for complexes **1** and **2**.

Figure 1 shows the low-temperature (−70 °C, CD_3OD) $^{31}P\{^1H\}$ NMR spectrum of the dmpe derivative **3a**. Three species, **3a-I**, **3a-II**, and **3a-III**, geometrically related by 90° turns of the CO_2 ligands around the Mo–CO_2 bond axis, are clearly present at measurable concentrations (2:1:2 ratio), two of which give rise to AA′XX′ patterns while the third, and less abundant, has nonequivalent ^{31}P nuclei and affords an AMQX set of lines (δ_A −2, δ_M 13.0, δ_Q 32.2, δ_X 42.3; $^2J_{AM}$ = 18 Hz, $^2J_{AQ}$ = 21 Hz, $^2J_{AX}$ = 158 Hz, $^2J_{MQ}$ = 156 Hz, $^2J_{MX}$ = 12 Hz, $^2J_{QX}$ = 0 Hz). The latter can be unequivocally assigned to the asymmetric rotamer **3a-II**, but an unambiguous assignment of the two AA′XX′ patterns to the disymmetric rotamers **3a-I** and **3a-III** cannot confidently be made. Fast interconversion of the three rotamers takes place at higher temperatures, a single AA′XX′ spin system being observed in the fast exchange limit (90 °C, $C_6D_5CD_3$). Under these conditions, the methyl groups of the two PMe_3 ligands give a doublet at 1.47 ppm ($^2J_{HP}$ = 6.5 Hz) in the ^1H NMR spectrum whereas the dmpe-methyl groups become equivalent two by two and yield separate doublets at δ 1.34 and 1.52 ($^2J_{HP}$ = 8 Hz).

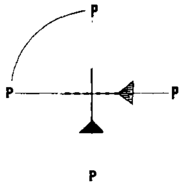

3-I

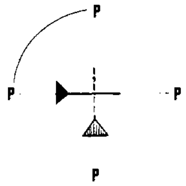

3-II

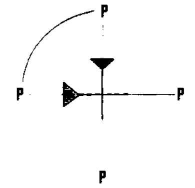

3-III

While the depe derivative **3b** exhibits a similar behavior, a somewhat simpler situation is found for the dmpm and dppe complexes, **3c** and **3d**, respectively. Thus **3c** exists at low temperature (CD_3OD, −90 °C) almost exclusively as the asymmetric isomer **3c-II**, the other two isomers accounting together for 10% of the total mixture. Isomer interconversion is fast at temperatures above 20 °C, and at 65 °C (THF) only one AA′XX′ spin system is observed. The assignment of the NMR parameters listed in the Experimental Section has been accomplished with the aid of selective decoupling experiments. Again, it is worth pointing out that in the fast exchange regime the methyl groups of the chelating phosphine ligand give rise to two separate doublets. For the dppe complex **3d**, only one species is observed at low temperatures. This gives rise to an AA′XX′ pattern in the $^{31}P\{^1H\}$ NMR spectrum (CD_3OD, −70 °C) and is therefore in accord with either structure **3d-I** or **3d-III**. Upon warming, the ^{31}P resonances broaden slightly until at 60 °C a well-defined AA′XX′ spin system is restored. No evidence for the existence of the other rotamers has been found although their presence is invoked to account for the observed fluxionality.

***trans*-Mo(CO$_2$)$_2$(P–P)$_2$ (4) Complexes.** Under somewhat more rigorous conditions (THF, 60 °C, 3 h) the two remaining PMe_3 ligands in compounds **3a** and **3b** can be substituted by a second molecule of the chelating diphosphine, eq 2. Compound **3c** does not afford a related complex, and in the case of **3d** a similar reaction has not been attempted in view of the thermal instability

$$\underset{\mathbf{3a,b}}{trans\text{-}Mo(CO_2)_2(P\text{–}P)(PMe_3)_2} \xrightarrow[\text{THF, 60 °C}]{\text{P–P}} trans\text{-}Mo(CO_2)_2(P\text{–}P)_2 + 2PMe_3 \quad (2)$$

P–P = dmpe (**4a**),
depe (**4b**)

---

[9] (a) March, J. *Advanced Organic Chemistry*; Wiley: New York, 1985; p 124. (b) Oki, M. *Applications of Dynamic NMR Spectroscopy to Organic Chemistry*; VCH Publishers: Weinheim, Germany, 1985; Chapter 7.

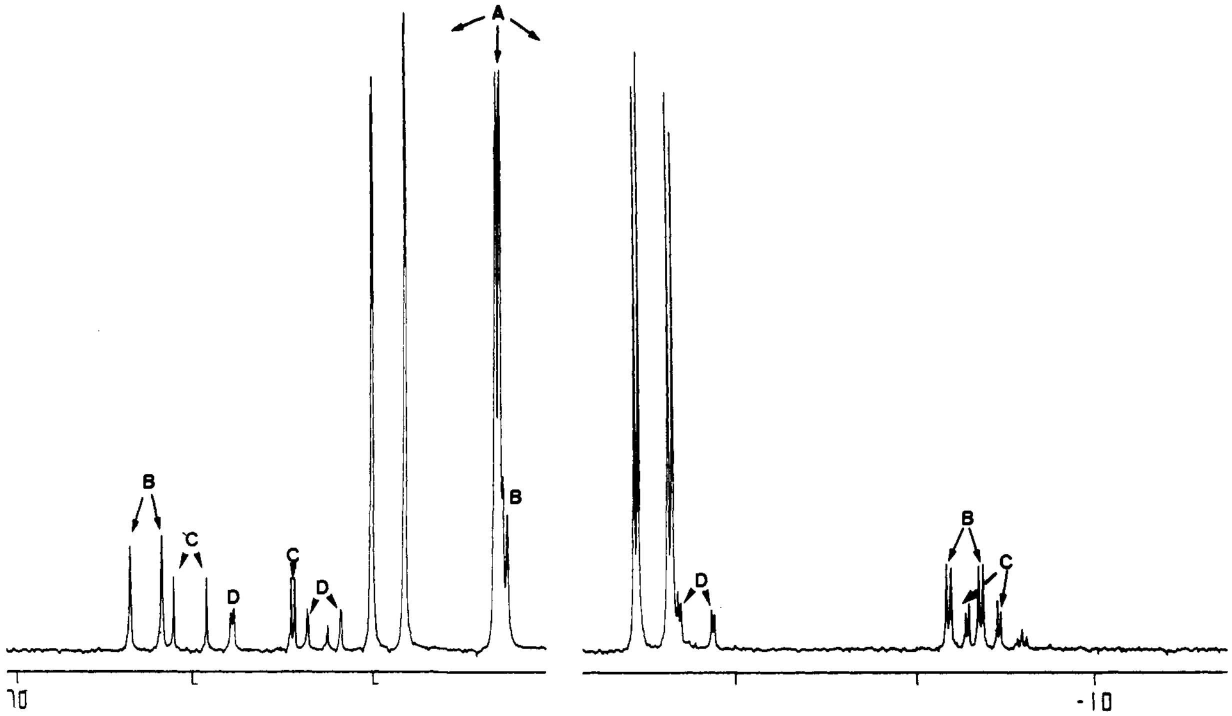

Figure 2. $^{31}P\{^1H\}$ NMR spectrum (CD_3OD, −70 °C) of complex **5a** showing the existence of four (A, B, C, and D) rotameric species.

reported for the complex *trans*-$Mo(CO_2)_2(dppe)_2$.[10]

The new compounds **4a** and **4b** display surprisingly high thermal stability and can be heated to 150 °C (mesitylene) without apparent decomposition. Two rotamers, **4-I** and **4-II**, are possible for these complexes, and both are indeed observed at low temperatures (CD_3OD, −60 °C, AA′XX′ patterns in a 3:2 ratio for **4a** and 3:1 for **4b**). Both rotamers interconvert on the NMR time scale at high temperatures and provide a sharp singlet ($W_{1/2}$ = 4–8 Hz) in the fast exchange regime (150 °C, mesitylene). Related changes are observed in the ^1H NMR spectra. Thus, for **4a**, at −25 °C, four methyl resonances can be detected for each rotamer in accord with their low-symmetry structures. In the fast exchange limit ($C_6D_5CD_3$, 75 °C) two pseudotriplets appear at 1.16 and 1.23 ppm ($J_{HP_{app}}$ = 3.2 Hz). Note that, under these conditions, the effective spin system for each type of methyl proton can be described as $A_3XX'A'_3$, with the strong coupling between the trans ^{31}P nuclei (X and X′) giving rise to the observed virtual coupling effects.[11]

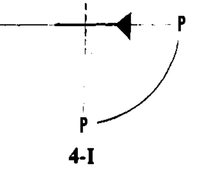

4-I

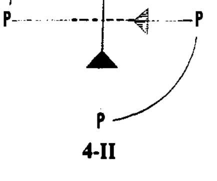

4-II

***trans*-$Mo(CO_2)_2$(P-P)(PMe_3)(CNR) (5) Complexes.** By taking advantage once more of the lability of the PMe_3 ligands in complexes **3**, the new compounds *trans*-$Mo(CO_2)_2$(depe)(PMe_3)(CNR) (R = Bu^t (**5a**), Cy (**5b**)) have been synthesized as depicted in eq 3. Compounds **5** are yellow crystalline solids with characteristic IR absorptions at 2110 (**5a**) and 2120 cm^{-1} (**5b**) due to the coordinated CNR ligand. Figure 2 shows the low-temperature (−70 °C, CD_3OD) $^{31}P\{^1H\}$ NMR spectrum of **5a** which consists of four AMX spin systems, one for each of the possible rotamers **5-I**–**5-IV**. For **5b** the corresponding low-temperature spectrum is further complicated by the expected axial–equatorial isomerism of the cyclohexyl residue,[9] which is responsible for the observation of two 1:1 AMX patterns for each rotamer. At appropriate temperatures the interconversion of these species is fast on the NMR time scale and a single AMX pattern is observed for both **5a** and **5b**. Due to the complexity of the system, no useful information could be obtained from a study of the variable-temperature ^1H NMR spectra of compounds **5**.

$$\underset{\mathbf{3b}}{trans\text{-}Mo(CO_2)_2(depe)(PMe_3)_2} + CNR \rightarrow$$
$$\rightarrow trans\text{-}Mo(CO_2)_2(depe)(PMe_3)(CNR) + PMe_3 \quad (3)$$
$$R = Bu^t\ (\mathbf{5a}),\ Cy\ (\mathbf{5b})$$

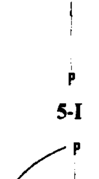

5-I

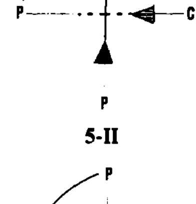

5-II

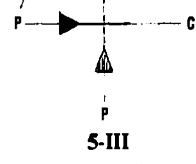

5-III

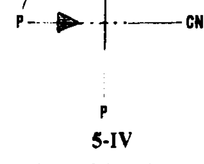

5-IV

Discussion

After having accomplished the synthesis and characterization of the first $(CO_2)_2$ adducts of a transition metal[3d] we set out to study their fluxional behavior. To deal with this problem we have taken advantage of the following facts: (i) The stability of the $Mo(CO_2)_2$ linkages in the parent complex *trans*-$Mo(CO_2)_2(PMe_3)_4$ (**1**) which, coupled with the lability of the PMe_3 ligands, has allowed the preparation of the new $(CO_2)_2$ complexes **2**–**5**, derived from **1** by substitution of one, two, three, or even four of the original PMe_3 groups. It should be pointed out that the above

---

[10] Chatt, J.; Hussain, W.; Leigh, G. J. *Trans. Met. Chem.* (*Weinheim, Ger.*) **1983**, *8*, 383.

[11] Harris, R. K. *Can. J. Chem.* **1964**, *42*, 2275.

Scheme I. Possible Intramolecular Pathways for the Fluxional Behavior of the Bis CO_2 Adducts of Molybdenum[a]

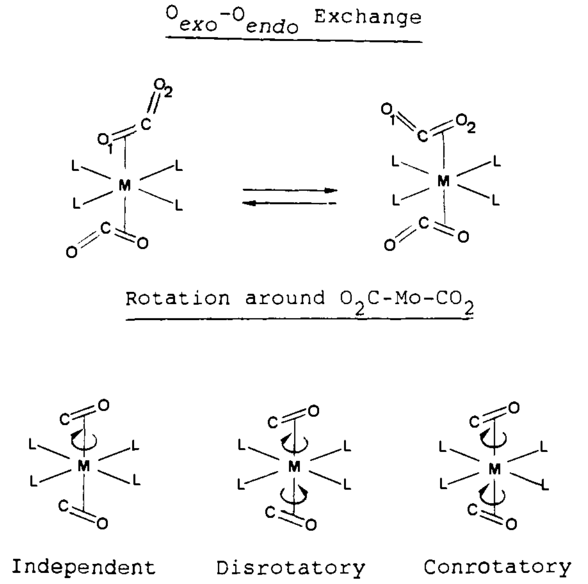

[a] The exo oxygen atoms of the CO_2 ligands have been omitted for clarity.

complexes cannot be prepared by reaction of CO_2 with the appropriate dinitrogen derivatives. For this transformation the disproportionation reaction is favored over the formation of the corresponding adducts.[12] (ii) For these less symmetric species, the existence of different isomers arising from the different orientations of the CO_2 ligands with respect to the *trans*-L–Mo–L vectors of the equatorial plane can be predicted. These have been observed and their interconversion has proved to be a very valuable mechanistic probe for the process under investigation. (iii) The high sensitivity of the ^{31}P nuclei to different chemical environments, i.e. their enhanced chemical shift dispersion, as compared to other NMR techniques, provides useful and otherwise inaccessible information about the nature of the species present in solutions of the above complexes. (iv) Finally, it should be stressed that the excellent solubility properties and astonishingly high thermal stability (see above) exhibited by these complexes greatly facilitate the investigation of the large temperature ranges in which they display dynamic behavior. Experimentally, we have found that the use of polar solvents like methanol, while keeping essentially unchanged the nature of the species present in solution without altering greatly their relative proportions, slows down the exchange process. While the reason for this behavior is not presently known, it justifies the use of CD_3OD for most of the low-temperature spectra while aromatic solvents have been employed for the investigation of the fast exchange regime.

As already noted, the parent complex **1** displays dynamic behavior in solution. Since the ^{31}P–$^{13}CO_2$ coupling is maintained in the fast exchange limit, an intermolecular process involving fast dissociation–re-association of CO_2 cannot be responsible for this behavior. Scheme I shows four different intramolecular pathways: (i) exchange of the free and coordinated oxygen atoms of one of the CO_2 ligands, (ii) independent rotation of the CO_2 ligands, (iii) concerted disrotatory motion of the two molecules of CO_2, i.e both rotate synchronously in opposite directions, and (iv) concerted conrotatory motion (both rotate in the same direction). In a recent theoretical contribution, Sánchez-Marcos and co-workers have addressed this problem and concluded, on the basis of the model system *trans*-$Mo(CO_2)_2(PH_3)_4$, that only the conrotatory mechanism (iv) provides a reasonably low kinetic barrier.[5] As already noted, in order to prove this assumption experimentally, the investigation of substituted, less symmetric complexes (e.g. **2–5**) was carried out.

Scheme II. C=O Exo and Endo Interchange As Applied to Compounds **2**[a]

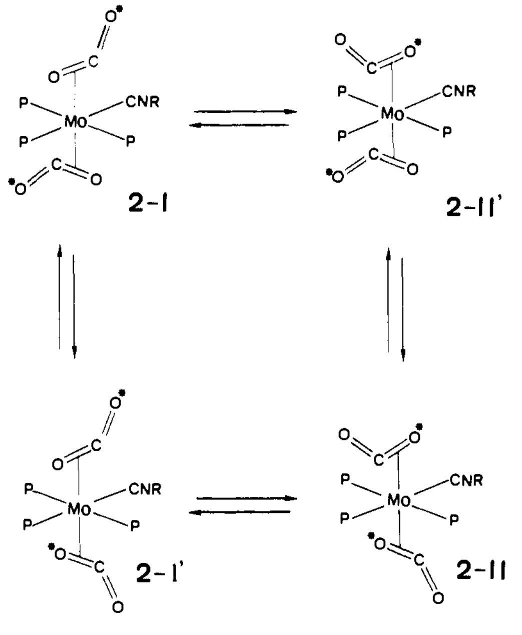

[a] The prime indicates enantiomeric structures.

Scheme III. Interchange of the Rotameric (and Enantiomeric) Structures of Compounds **3** by the Independent Rotation Mechanism[a]

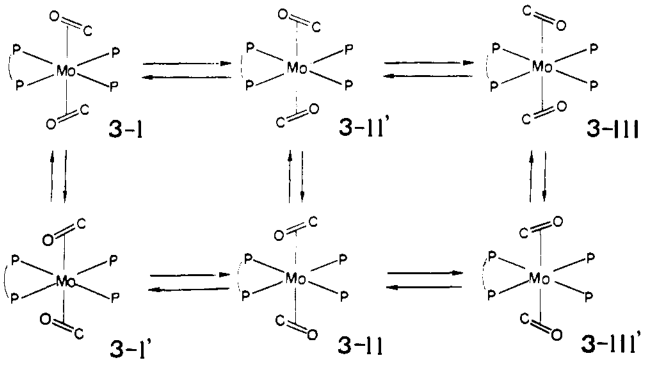

[a] The exo oxygen atoms of the CO_2 ligands have been omitted for clarity. The prime indicates enantiomeric structures.

Mechanism (i) postulates an intramolecular exchange of the free and coordinated C=O bonds of one of the CO_2 ligands. This could involve the intermediacy of an η^1-CO_2 complex,[3e,13] or alternatively it could occur by a concerted metal 1,2-shift similar to that invoked for the related change in transition-metal–allene complexes.[14] Application of this mechanism to complexes **2–5** accounts for the interconversion of the corresponding isomers as shown in Scheme II for compounds **2** taken as a representative example. This mechanism also explains the observation of two sets of resonances for the methyl protons of the chelating phosphine ligands in compounds **3** and **4** but fails to account for the observed equivalency of the two CO_2 ligands of the molecules of **2** in the fast exchange regime (see Results) and can therefore be disregarded on this basis.

The independent rotation of the CO_2 ligands, i.e. mechanism ii, can be easily discarded with reference to data obtained for compounds **3**. Scheme III shows the result of this process, which, as can be seen, allows the interconversion of the three rotamers,

---

[12] Alvarez, R.; Atwood, J. L.; Carmona, E.; Pérez, P. J.; Poveda, M. L.; Rogers, R. D. *Inorg. Chem.* **1991**, *30*, 1493.

[13] In the present system this seems to be an unfavorable electronic situation, very likely unaccessible at normal temperatures. See: Mealli, C.; Hoffmann, R.; Stockis, A. *Inorg. Chem.* **1984**, *23*, 56.

[14] Foxman, B.; Marten, D.; Rosan, A.; Raghu, S.; Rosenblum, M. *J. Am. Chem. Soc.* **1977**, *99*, 2160.

Scheme IV. The Disrotatory Mechanism As Applied to Compounds **2**[a]

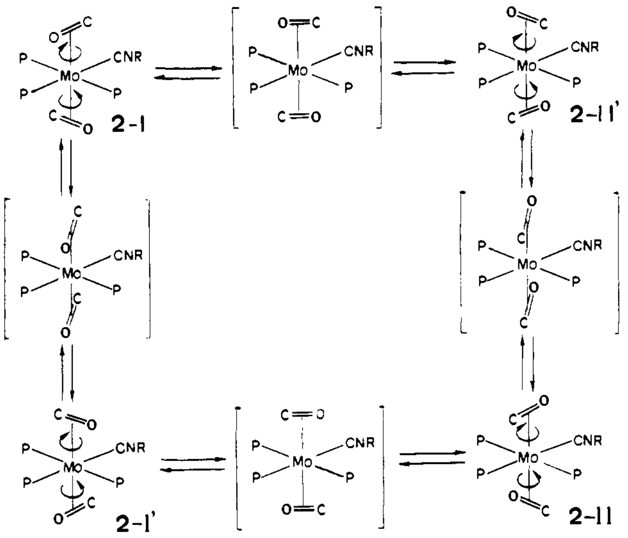

[a] The arrows indicate the sense of rotation of the CO_2 ligands when following the scheme clockwise. The exo oxygen atoms of the CO_2 ligands have been omitted for clarity. The prime indicates enantiomeric structures.

3-I, **3-II**, and **3-III**. This motion would involve at some stage a transition state, or an intermediate, that would introduce an effective plane of symmetry, as a result of an eclipsed distribution of the CO_2 ligands (see example C; the exo oxygen atoms have been omitted for clarity). Hence, the observation of two different resonances for the methyl groups of the chelating diphosphine ligands clearly stands against this mechanistic proposal.

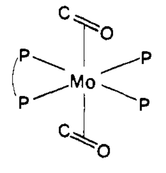

C

Of the several pieces of information that argue against the disrotatory motion (mechanism iii), two can be mentioned here. A clear picture of the effects of this mechanism is obtained when it is applied to the isocyanide complexes **2** (Scheme IV) or to the bis(chelating phosphine) compounds **4** (Scheme V). In the first instance this mechanism allows the interconversion of rotamers **2-I** and **2-II**, as well as their conversion into their enantiomers, **2-I′** and **2-II′**, respectively, but the two trans PMe_3 groups within each rotamer do not undergo site exchange and therefore maintain their inequivalency throughout this process. In the high-temperature limit an AMX spin system is to be expected for the phosphorus nuclei instead of the AX_2 pattern that is in fact observed for all of the complexes of type.[3d] As for compounds **4** (Scheme IV), the disrotatory motion converts either rotamer, **4-I** or **4-II**, into itself or into its corresponding enantiomer, **4-I′** or **4-II′**, respectively. Hence, no interconversion of rotamers **4-I** ⇌ **4-II** is to be expected in the fast exchange regime; this contrast with the observation of a sharp singlet in the $^{31}P\{^1H\}$ NMR spectra of **4a** and **4b** recorded at 150 °C (see Results).

We are finally left with the conrotatory motion, the only mechanism which satisfactorily fits the experimental data obtained for compounds **2-5**. Its effects, with reference to compounds **2** and **4**, are shown in Schemes VI and VII , respectively. Some important consequences of this process are as follows: (i) since the coordinated CO_2 ligands never eclipse each other, the equatorial plane, i.e. the plane perpendicular to the *trans*-O_2C–Mo–CO_2 bond axis, never becomes an effective plane of symmetry, (ii) in complexes **2** (i.e *trans*-$Mo(CO_2)_2(PMe_3)_3(CNR)$), equilibration of the CO_2 ligands becomes feasible through a transition state, or intermediate, of the type depicted in **D**, which possesses a binary axis of symmetry.

Scheme V. Disrotatory Motion of the CO_2 Ligands[a]

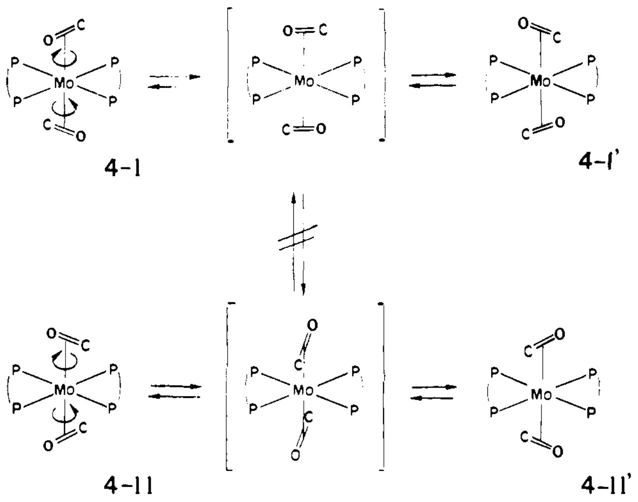

[a] The exo oxygen atoms of the CO_2 ligands have been omitted for clarity. The prime indicates enantiomeric structures.

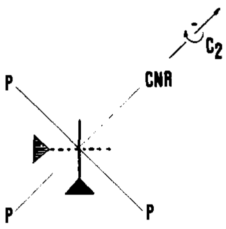

D

As a result of the above, the following predictions can be made for the fast exchange regime of complexes **2-5**: (a) the different rotamers expected for each type of complex should interconvert (although no interconversion of enantiomeric structures must take place), (b) the methyl groups of the chelating phosphines in complexes **3** and **4** should arrange in two sets, and (c) the two CO_2 ligands in compounds **2** should become equivalent. In addition, the exchange rate of the trans ^{31}P nuclei in both rotamers **2-I** and **2-II** need not be the same. These expectations are fully met by the experimental data, and therefore it can be concluded that the process responsible for the fluxionality of complexes **1-5** is the conrotatory motion of the coordinated CO_2 ligands. A line-shape analysis carried out with complex **4a** is also in accord with this proposal. Details of this study are given in the Experimental Section, while Figure 3 shows the experimental and the simulated spectra. Due to the strongly second-order nature of the spectra, the simulated line shapes in the intermediate regime were strongly dependent on the exact coupling constants used in the simulations. The imperfect fits of the experimental and simulated data are due to the difficulty of determining the coupling constants with sufficient accuracy.

Conclusions

The reluctance of the CO_2 ligands in these $Mo(CO_2)_2$ adducts to undergo substitution reactions, coupled with the lability of the PMe_3 groups, has allowed the synthesis of new bis(carbon dioxide) complexes of composition *trans*-$Mo(CO_2)_2(P{-}P)(PMe_3)_2$ (**3**), *trans*-$Mo(CO_2)_2(P{-}P)_2$ (**4**), and *trans*-$Mo(CO_2)_2$(depe)-$(PMe_3)(CNR)$ (**5**). The strength of the Mo–CO_2 linkages in these compounds is further demonstrated by the surprisingly high thermal stability exhibited by some of these complexes (specially compounds **4**, which are stable at least up to 150 °C in solution). The above compounds, as well as the related *trans*-$Mo(CO_2)_2(PMe_3)_3(CNR)$ (**2**), have been shown to exist in solution as thermodynamic mixtures of isomers arising from the different geometrical distributions of the non-symmetric coordinated CO_2

Scheme VI. Application of the Conrotatory Mechanism to Compounds **2**[a]

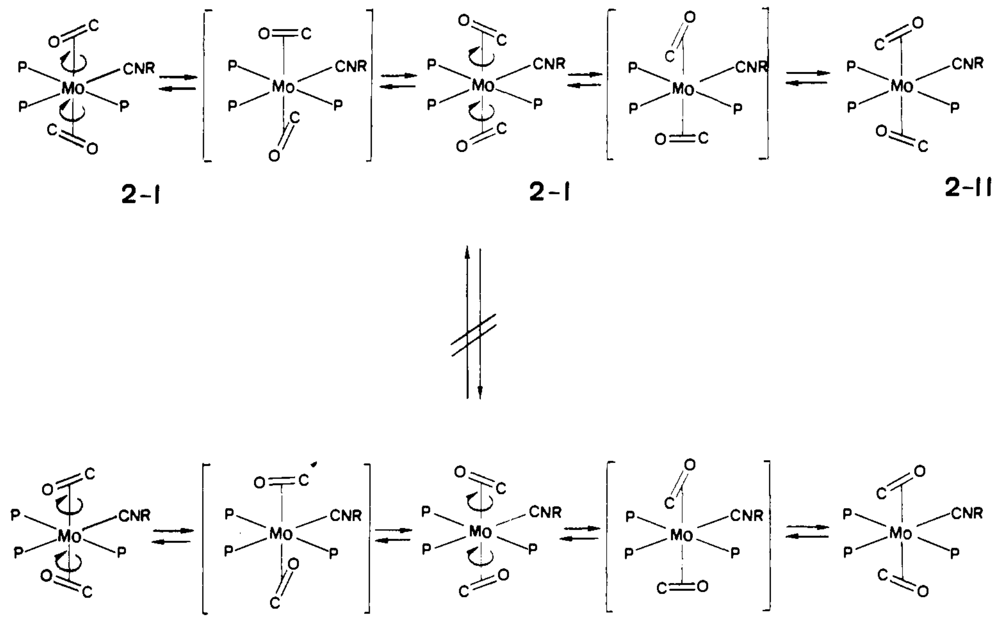

[a]The exo oxygen atoms of the CO_2 ligands have been omitted for clarity. The prime indicates enantiomeric structures.

Scheme VII. The Interchange of Rotamers **4** by Conrotatory Rotation of the CO_2 Ligands[a]

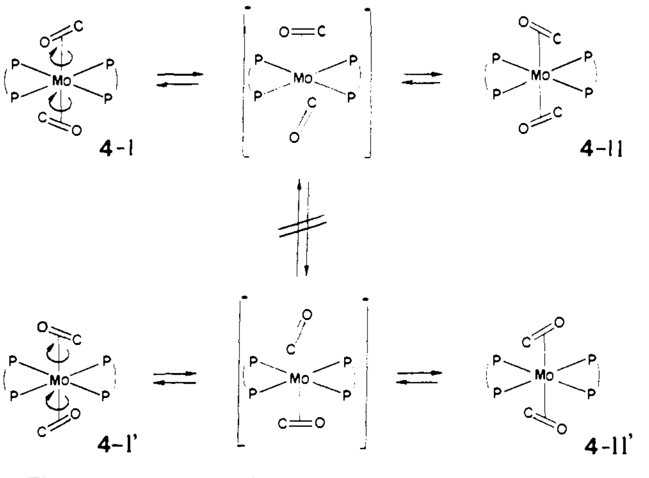

[a]The exo oxygen atoms of the CO_2 ligands have been omitted for clarity. The prime indicates enantiomeric structures.

ligands. These isomers interconvert in solution by a synchronous motion of the CO_2 ligands in which both molecules rotate in the same direction. Since this motion does not exchange enantiomeric structures, the possibility of isolating optically active $(CO_2)_2$ adducts can confidently be expected.

Experimental Section

Microanalyses were carried out by Pascher Microanalytical Laboratory, Remagen (Germany), and the Analytical Service of the University of Sevilla. Infrared spectra were recorded on Perkin-Elmer Models 577 and 684 spectrophotometers. ^1H, ^{31}P, and ^{13}C NMR spectra were run on a Varian XL-200 spectrometer. ^{31}P shifts were measured with respect to external 85% H_3PO_4. ^{13}C NMR spectra were referenced by using the ^{13}C resonance of the solvent as an internal standard but are reported with respect to $SiMe_4$.

All preparations and other operations were carried out under oxygen-free nitrogen following conventional Schlenk techniques. Solvents were dried and degassed before use. The petroleum ether used had a boiling point range of 40–60 °C. The compounds *trans*-$Mo(CO_2)_2(PMe_3)_4$ and *trans,mer*-$Mo(CO_2)_2(PMe_3)_3(CNR)$ (R = Bu^t, Cy) were prepared according to the literature procedures.[3d] PMe_3 was obtained by the method of Wolfsberger and Schmidbaur[15] and the ligands dmpm, dmpe, and depe were prepared by treating the tetrachlorides $Cl_2P(CH_2)_nPCl_2$ (n = 1, 2) with 4–5 equiv of the corresponding Grignard reagents.

NMR Spectroscopic Data for $Mo(CO_2)_2(PMe_3)_3(CNR)$ (2) Complexes. Since only NMR data corresponding to the fast exchange limit have been originally reported[3d] for compounds **2**, for the sake of completeness a full account, including variable-temperature data, is given below. $Mo(CO_2)_2(PMe_3)_3(CNBu^t)$ (**2a**): ^1H NMR (200 MHz, C_6D_6, 20 °C) δ 1.17 (d, 9 H, PMe_3, $^2J_{HP} = 6.5$ Hz), 1.22 (s, 9 H, CMe_3), 1.40 (pseudotriplet, 18 H, 2 PMe_3, $J_{HPapp} = 3$ Hz). $^{31}P\{^1H\}$ NMR (CD_3OD, −90 °C) two AMX spin systems. Major isomer, δ_A −4.7, δ_M −2.6, δ_X 15.0, $^2J_{AM} = 23$ Hz, $^2J_{AX} = 16$ Hz, $^2J_{MX} = 148$ Hz. Minor isomer δ_A −4.8, δ_M 11.5, δ_X 16.5, $^2J_{AM} = 150$ Hz, $^2J_{AX} = 20$ Hz, $^2J_{MX} = 14$ Hz. Isomer ratio $\simeq$ 6:1. $^{31}P\{^1H\}$ NMR (C_6D_6, 45 °C) AX_2 spin system, δ_A −8.4, δ_X 0.4, $^2J_{AX} = 19$ Hz. $^{13}C\{^1H\}$ NMR (30% $^{13}CO_2$-enriched sample, CD_3OD, −90 °C) δ 210. 7 (dt, 1 CO_2, $^2J_{CP} = 41$ and 9 Hz), 213.5 (dt, 1 CO_2, $^2J_{CP} = 16, 10$ Hz). $^{13}C\{^1H\}$ NMR (30% $^{13}CO_2$-enriched sample, CD_3OD, 20 °C) δ 210.4 (td, CO_2, $^2J_{CP} = 19, 13$ Hz). $Mo(CO_2)_2(PMe_3)_3(CNCy)$ (**2b**): ^1H NMR (200 MHz, C_6D_6, 20 °C) δ 1.10 (d, 9 H, PMe_3, $^2J_{HP} = 6.5$ Hz), 1.36 (pseudotriplet, 18 H, 2 PMe_3, $J_{HPapp} = 3$ Hz), 1.53 and 3.31 (br, C_6H_{11}). $^{31}P\{^1H\}$ NMR (CD_3OD, −90 °C) two predominant AMX spin systems (conformers, see Results), δ_A −4.7, δ_M −2.4, δ_X 15.1, $^2J_{AM} = 23$ Hz, $^2J_{AX} = 18$ Hz, $^2J_{MX} = 143$ Hz; δ_A −4.7, δ_M −2.8, δ_X 14.9, $^2J_{AM} = 23$ Hz, $^2J_{AX} = 18$ Hz, $^2J_{MX} = 143$ Hz. Conformer ratio $\simeq$ 1:1. Most of the resonances corresponding to the mixture of conformers for the minor rotamer are obscured by the main signals of the predominant species, and therefore their characteristic data are not reported. Rotamer ratio $\simeq$ 6:1.

Synthesis of *trans*-$Mo(CO_2)_2(P\text{-}P)(PMe_3)_2$ Complexes. To a solution of *trans*-$Mo(CO_2)_2(PMe_3)_4$ (0.49 g, 1 mmol) in 40 mL of THF was added a slight excess of dmpe (0.15 mL, 1.5 mmol) via syringe. The resulting mixture was stirred at room temperature for 20 min ($^{31}P\{^1H\}$ NMR analysis indicates quantitative transformation of **1** into **3a**) and the volatiles were removed under vacuum. Extraction with 25 mL of Et_2O, centrifugation, partial removal of the solvent, and cooling at −30 °C produced complex **3a** as a very pale yellow crystalline material in 60% yield.

Following a similar procedure the depe (**3b**) and dmpm (**3c**) derivatives were obtained (yellow crystals from Et_2O–petroleum ether and orange crystals from toluene, respectively) in 60% yield. The formation of the corresponding dppe derivative (**3d**) proceeded more slowly, and 4 days of stirring in THF were needed to achieve complete formation. After the mixture was taken to dryness, the residue was extracted with THF (30 mL) and centrifuged. Upon cooling at −30 °C complex **3d** was obtained in 50% yield in the form of a yellow microcrystalline solid.

---

[15] Wolfsberger, W.; Schmidbaur, H. *Synth. React. Inorg. Metal-Org. Chem.* **1974**, *4*, 149.

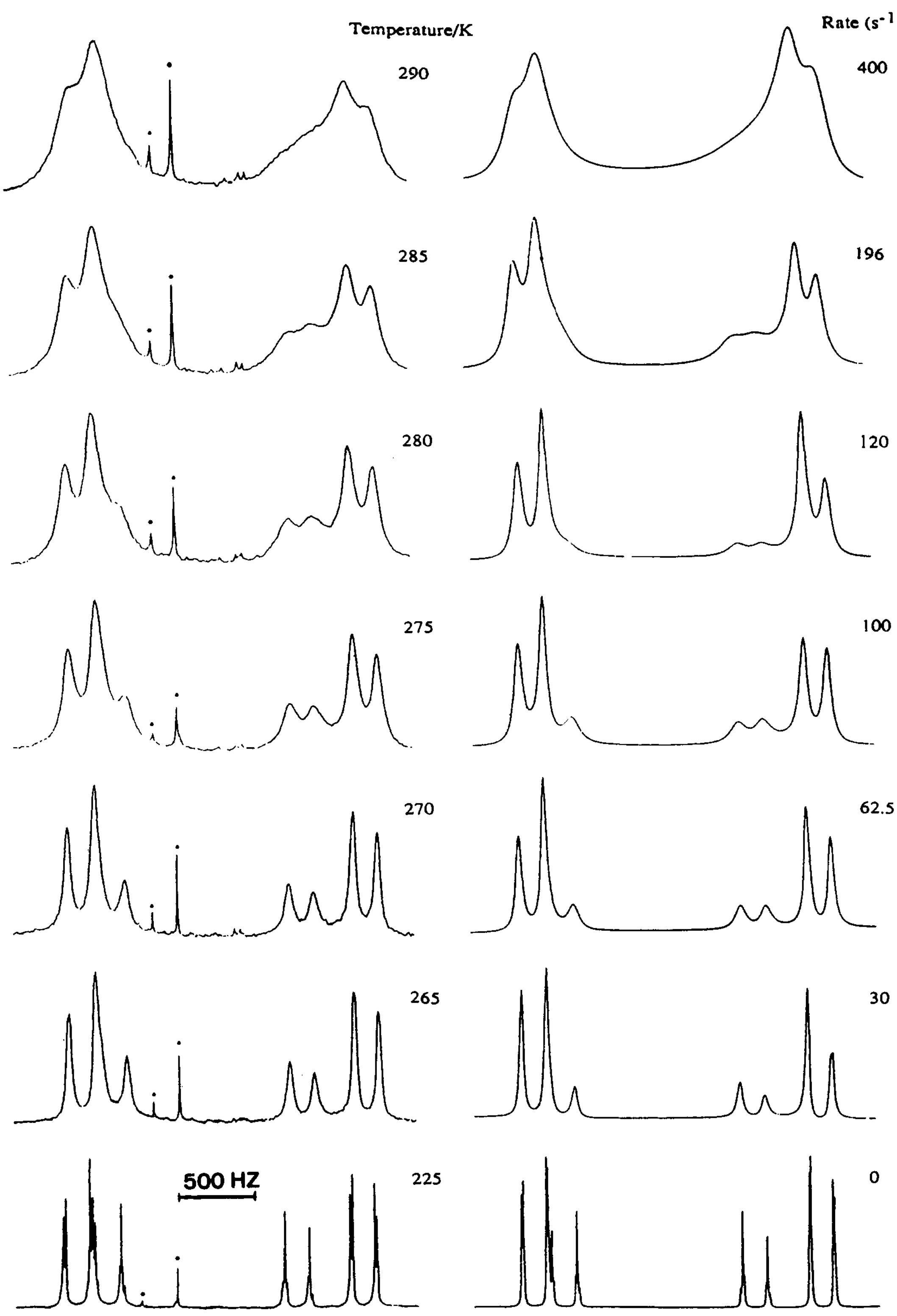

Figure 3. Left: Experimental $^{31}P\{^1H\}$ variable-temperature NMR spectra ($C_6D_5CD_3$, 121.49 MHz) of complex **4a**. The dots indicate some minor impurities. Right: Best fit, computer-simulated $^{31}P\{^1H\}$ spectra for the conrotatory motion of the two CO_2 ligands.

$Mo(CO_2)_2(dmpe)(PMe_3)_2$ (**3a**): IR (Nujol mull) 1660 (s), 1155 (m), 1100 cm^{-1} (m) (CO_2 absorptions). ^1H NMR (200 MHz, CD_3OD, 60 °C) δ 1.34 (d, 6 H, 2 Me, dmpe, $^2J_{HP}$ = 8 Hz), 1.48 (d, 18 H, 2 PMe_3, $^2J_{HP}$ = 6.8 Hz), 1.52 (d, 6 H, 2 Me, dmpe, $^2J_{HP}$ = 8 Hz). $^{31}P\{^1H\}$ NMR (CD_3OD, −70 °C) two major AA′XX′ spin systems, δ_A −3.5 (PMe_3), δ_X 45.5 (dmpe) and δ_A 13.6 (PMe_3), δ_X 31.4 (dmpe). Minor AMQX spin system, δ_A −2.7 (PMe_3), δ_M 13.0 (PMe_3), δ_Q 32.2 (dmpe), δ_X 42.3 (dmpe), $^2J_{AM}$ = 18 Hz, $^2J_{AQ}$ = 21 Hz, $^2J_{AX}$ = 158 Hz, $^2J_{MQ}$ = 156 Hz, $^2J_{MX}$ = 12 Hz, $^2J_{QX}$ = 0 Hz. Isomer ratio $\simeq$ 2:2:1. $^{31}P\{^1H\}$ NMR ($C_6D_5CD_3$, 90 °C) AA′XX′ spin system, δ_A −3.0 (PMe_3), δ_X 38.4 (dmpe). $^{13}C\{^1H\}$ NMR (C_6D_6, 20 °C) δ 12.1 (d, 2 Me, dmpe, $^1J_{CP}$ = 16 Hz), 13.2 (br d, 2 Me, dmpe, $^1J_{CP}$ = 20 Hz), 17.5 (d, PMe_3, $^1J_{CP}$ = 18 Hz), 27.9 (d, CH_2P, $^1J_{CP}$ = 26 Hz), 28.2 (d, CH_2–P, $^1J_{CP}$ = 27 Hz). Anal. Calcd for **3a**: C, 34.3; H, 7.0. Found: C, 34.6; H, 7.0.

$Mo(CO_2)_2$(depe)$(PMe_3)_2$ (3b): IR (Nujol mull) 1670 (s), 1155 (m), 1100 cm^{-1} (m) (CO_2 absorptions). ^1H NMR (200 MHz, CD_3OD, 20 °C) δ 1.21 (complex m, depe), 1.48 (d, PMe_3, $^2J_{HP}$ = 7.6 Hz). $^{31}P\{^1H\}$ NMR (CD_3OD, −80 °C) two major AA′XX′ spin systems, δ_A −3.7 (PMe_3), δ_X 54.9 (depe) and δ_A 15.0 (PMe_3), δ_X 39.5 (depe). Minor AMQX spin system, δ_A −3.9 (PMe_3), δ_M 14.6 (PMe_3), δ_Q 42.8 (depe), δ_X 54.8 (depe), $^2J_{AM}$ = 18 Hz, $^2J_{AQ}$ = 17 Hz, $^2J_{AX}$ = 152 Hz, $^2J_{MQ}$ = 147 Hz, $^2J_{MX}$ = 10, $^2J_{QX}$ = 0 Hz. Isomer ratio $\simeq$ 2:2:1. $^{31}P\{^1H\}$ NMR ($C_6D_5CD_3$, 90 °C) AA′XX′ spin system, δ_A 0.8 (PMe_3), δ_X 46.5 (depe). Anal. Calcd for **3b**: C, 39.9; H, 7.7. Found: C, 39.8; H, 7.7.

$Mo(CO_2)_2$(dmpm)$(PMe_3)_2$ (3c): IR (Nujol mull) 1660 (s), 1150 (m), 1100 cm^{-1} (m) (CO_2 absorptions). ^1H NMR (200 MHz, CD_3OD, −80

°C) major isomer, δ 1.11 (d, 3 H, Me of dmpm, $^2J_{HP} = 8.5$ Hz), 1.39 (d, 9 H, PMe_3, $^2J_{HP} = 10$ Hz), 1.44 (d, 9 H, PMe_3, $^2J_{HP} = 8$ Hz), 1.52 (d, 3 H, Me of dmpm, $^2J_{HP} = 7.3$ Hz), 1.59 (d, 3 H, Me of dmpm, $^2J_{HP} = 8$ Hz), 1.92 (d, 3 H, Me of dmpm, $^2J_{HP} = 9.2$ Hz), 3.85 (complex m, 2 H, CH_2–P). ^1H NMR (CD_3OD, 60 °C) δ 1.40 (d, 18 H, 2 PMe_3, $^2J_{HP} = 7.8$ Hz), 1.47 (d, 6 H, 2 Me of dmpm, $^2J_{HP} = 8$ Hz), 1.60 (d, 6 H, 2 Me of dmpm, $^2J_{HP} = 8.4$ Hz), 3.54 (tt, 2 H, CH_2–P, $^2J_{HP} = 10$ Hz, $^4J_{HP} = 1$ Hz). $^{31}P\{^1H\}$ NMR (CD_3OD, −90 °C) major AMQX spin system, δ_A −18.8, δ_M −1.1, δ_Q 3.8, δ_X 22.0, $^2J_{AM} = 0$ Hz, $^2J_{AQ} = 25$ Hz, $^2J_{AX} = 157$ Hz, $^2J_{MQ} = 157$ Hz, $^2J_{MX} = 18$ Hz, $^2J_{QX} = 16$ Hz. Minor AA′XX′ spin system, δ_A −20.0 (dmpm), δ_X 19.6 (PMe_3). Major to minor isomer ratio ≃ 9. $^{31}P\{^1H\}$ NMR (THF, 60 °C) AA′XX′ spin system, δ_A −9.8 (dmpm), δ_X 6.7 (PMe_3). The assignment has been confirmed by selective ^1H decoupling experiments. Anal. Calcd for **3c**: C, 32.8; H, 6.6. Found: C, 33.1; H, 6.8.

Mo(CO$_2$)$_2$(dppe)(PMe$_3$)$_2$ (3d): IR (Nujol mull) 1680 (s), 1660 (s), 1150 (m), 1110 cm^{-1} (m) (CO_2 absorptions). ^1H NMR (200 MHz, CD_3OD, 20 °C) δ 1.24 (d, 18 H, 2 PMe_3, $^2J_{HP} = 8.6$ Hz), 2.25 and 2.86 (m, 4 H, CH_2–P), 7.33–7.87 (m, aromatics). $^{31}P\{^1H\}$ NMR (CD_3OD, −70 °C) AA′XX spin system, δ_A 18.3 (PMe_3), δ_X 36.6 (dppe). Anal. Calcd for **3d**: C, 56.8; H, 6.3. Found: C, 55.6; H, 5.7.

Synthesis of *trans*-Mo(CO$_2$)$_2$(P–P)$_2$ Complexes. Dmpe (0.5 mL, 2.5 mmol) was added to a solution of complex **1** (0.49 g, 1 mmol) in THF (30 mL). The resulting mixture was heated, with stirring, at 60 °C for 3 h, the volatiles were removed under vacuum, and the residue was washed with Et_2O, extracted with 20 mL of toluene, and centrifuged. Complex **4a** crystallized as a yellow solid by cooling at −30 °C. Yield 50%.

Under similar reaction conditions, complex **4b** can be obtained in 60% yield as yellow crystals from Et_2O–petroleum ether.

Mo(CO$_2$)$_2$(dmpe)$_2$ (4a): IR (Nujol mull) 1650 (s), 1150 (m), 1100 cm^{-1} (m) (CO_2 absorptions). ^1H NMR (200 MHz, CD_3OD, −25 °C) major isomer δ 0.93, 1.47, 1.50, and 1.97 (d, d, d, dd, 1:1:1:1 ratio, MeP, $^2J_{HP} = 8$ Hz, $^2J_{HP} = 7.4$ Hz, $^2J_{HP} = 8$ Hz, $^2J_{HP} = 9$ Hz and $^4J_{HP} = 1.2$ Hz, respectively). Minor isomer, δ 0.90, 1.35, 1.65, and 1.96 (d, d, d, d, 1:1:1:1 ratio, Me–P, $^2J_{HP} = 7$, 7.7, 7.8, 9.1 Hz, respectively). Isomer ratio ≃ 1.5:1. ^1H NMR (C_6D_6, 70 °C) δ 1.16 and 1.23 (pseudotriplets, 1:1 ratio, Me–P, $J_{HPapp} = 3.2$ Hz), 1.4 (broad hump, CH_2–P). $^{31}P\{^1H\}$ NMR (CD_3OD, −20 °C) two AA′XX′ spin systems in a 3:2 ratio, δ_A 33.7, δ_X 47.4 and δ_A 37.4, δ_X 46.3, respectively. $^{31}P\{^1H\}$ NMR ($C_6D_5CD_3$–mesitylene, 150 °C) δ 37.8 (s), $W_{1/2} = 4$ Hz. Anal. Calcd for **4a**: C, 35.1; H, 6.7. Found: C, 34.7; H, 6.6.

Mo(CO$_2$)$_2$(depe)$_2$ (4b): IR (Nujol mull) 1660 (s), 1150 (m), 1100 cm^{-1} (m) (CO_2 absorptions). $^{31}P\{^1H\}$ NMR (CD_3OD, −60 °C) two AA′XX′ spin systems in a 3:1 ratio, δ_A 46.4, δ_X 54.7 and δ_A 46.5, δ_X 57.6, respectively. $^{31}P\{^1H\}$ NMR ($C_6D_5CD_3$–mesitylene, 145 °C) δ 50.7 (s), $W_{1/2} = 8$ Hz. Anal. Calcd for **4b**: C, 44.3; H, 8.1. Found: C, 44.3; H, 8.0.

Line-Shape Analysis of 4a. The 121.49 MHz $^{31}P\{^1H\}$ NMR spectra used for this study have been recorded on a Bruker AM-300 instrument at the University of Oxford over the temperature range −58 to 22 °C. The low-temperature limiting spectrum was recorded at high resolution with good signal-to-noise ratio and was simulated using PANIC[16] in order to provide accurate chemical shifts and coupling constants. These values were then used as inputs to the DNMR4 simulation program.[17] The spectra were recorded in $C_6D_5CD_3$ as a solvent and characterized by the following NMR parameters (chemical shifts relative to trimethylphosphate, $(MeO_3)_3PO$): rotamer ratio ≃ 2:1. Major isomer δ_A 42.1, δ_X 27.0; $^2J_{AX} = 155$ Hz, $^2J_{A'X} = -12$ Hz, $^2J_{AA'} = -2$ Hz, $^2J_{XX'} = -2$ Hz. Minor isomer δ_A 40.6, δ_X 30.6; $^2J_{AX} = 160.3$ Hz, $^2J_{A'X} = -3$ Hz, $^2J_{AA'} = 13.2$ Hz, $^2J_{XX'} = 13.2$ Hz. The experimental spectra are illustrated in Figure 3 together with the simulated spectra for the conrotatory model. The gross similarities of the simulated and experimental spectra confirm our findings based on the multiplicity of the NMR resonances and the symmetries that these imply for the transition states (see Discussion). An Arrhenius plot (ln *k* vs 1/*T*) gave a straight line and the following values for the activation parameters (300 K): $\Delta H^{*} = 58$ kJ·mol^{-1}; $\Delta S^{*} = 20$ J·K^{-1}·mol^{-1}.

Synthesis of Mo(CO$_2$)$_2$(depe)(PMe$_3$)(CNR) Complexes. A solution of complex **3b** (0.2 g, 0.35 mmol) in THF (30 mL) was treated with 1 equiv of the corresponding isocyanide. After heating at 40 °C for 12 h the resulting mixture was evaporated to dryness, extracted with a mixture of Et_2O–petroleum ether, and centrifuged. With cooling to −30 °C complexes **5a** (R = Bu^t) and **5b** (R = Cy) were obtained as yellow crystalline solids in 60–70% yield.

Mo(CO$_2$)$_2$(depe)(PMe$_3$)(CNBu^t) (5a): IR (Nujol mull) 2110 (s) (CN), 1710 (s), 1690 (s), 1160 (m), 1105 cm^{-1} (m) (CO_2 absorptions). ^1H NMR (200 MHz, CD_3OD, 60 °C) δ 1.52 (d, 9 H, PMe_3, $^2J_{HP} = 8.7$ Hz), 1.59 (s, 9 H, CMe_3), 1.1–2.0 (complex multiplets, depe). $^{31}P\{^1H\}$ NMR (CD_3OD, −70 °C) four AMX spin systems. Major isomer, δ_A 14.4 (PMe_3), δ_M 42.9 (depe), δ_X 49.1 (depe), $^2J_{AM} = 18$ Hz, $^2J_{AX} = 147$ Hz, $^2J_{MX} = 6$ Hz. Minor isomers δ_A −2.7 (PMe_3), δ_M 42.5 (depe), δ_X 62.5 (depe), $^2J_{AM} = 23$ Hz, $^2J_{AX} = 148$ Hz, δ_A −3.7 (PMe_3), δ_M 52.6 (depe), δ_X 57.7 (depe), $^2J_{AM} = 147$ Hz, $^2J_{AX} = 16$ Hz, $^2J_{MX} = 4$ Hz; δ_A 12.0 (PMe_3), δ_M 54.3 (depe), δ_X 60.0 (depe), $^2J_{AM} = 13$ Hz, $^2J_{AX} = 150$ Hz. Isomer ratio ≃ 14:2:1:1, respectively. $^{31}P\{^1H\}$ NMR (CD_3OD, 65 °C) AMX spin system, δ_A 7.3 (PMe_3), δ_M 46.3 (depe), δ_X 53.0 (depe), $^2J_{AM} = 16$ Hz, $^2J_{AX} = 150$. Anal. Calcd for **5a**: C, 43.5; H, 7.8. Found: C, 43.7; H, 7.7.

Mo(CO$_2$)$_2$(depe)(PMe$_3$)(CNCy) (5b): IR (Nujol mull) 2120 (s) (CN), 1710 (s), 1680 (s), 1160 (m), 1105 cm^{-1} (m) (CO_2 absorptions). $^{31}P\{^1H\}$ NMR (CD_3OD, −90 °C) two predominant AMX spin systems (conformers), δ_A 15.5 (PMe_3), δ_M 43.8 (depe), δ_X 49.9 (depe), $^2J_{AM} = 18$ Hz, $^2J_{AX} = 147$ Hz, $^2J_{MX} = 7$ Hz; δ_A 15.8 (PMe_3), δ_M 44.4 (depe), δ_X 49.9 (depe), $^2J_{AM} = 18$ Hz, $^2J_{AX} = 147$ Hz, $^2J_{MX} = 7$ Hz. Conformer ratio ≃ 1:1. Two minor AMX spin systems (conformers), δ_A − 1.8 (PMe_3), δ_M (obscured by the main rotamer), δ_X 63.6 (depe), $^2J_{AM} = 17$ Hz, $^2J_{AX} = 146$ Hz; δ_A −1.5 (PMe_3), δ_M (obscured by the main rotamer), δ_X 64.0 (depe), $^2J_{AM} = 17$ Hz, $^2J_{AX} = 146$ Hz. Conformer ratio ≃ 1:1. Rotamer ratio ≃ 2.5:1. $^{31}P\{^1\}$ NMR ($C_6D_5CD_3$, 90 °C): AMX spin system, δ_A 7.7 (PMe_3), δ_M 45.8 (depe), δ_X 56.3 (depe), $^2J_{AM} = 18$ Hz, $^2J_{AX} = 153$. Anal. Calcd for **5b**: C, 45.9; H, 7.8. Found: C, 45.9; H, 7.6.

Acknowledgment. We thank the Spanish Ministry of Education (M.A.M. and P.J.P.) and the SERC (A.K.H.) for research studentships. We gratefully acknowledge generous financial support from the Dirección General de Investigación Científica y Técnica (Proyecto PB86-0653) and Junta de Andalucía. Thanks are also due to the University of Sevilla for use of analytical and NMR facilities.

---

(16) *Parameter Adjustment in NMR Iterative Calculation*; Bruker NMR software manual.

(17) DNMR4, Quantum Chemical Program Exchange, Indiana University, QCPE program No. 466.